Research Article

Mechanical and Thermal Properties of Hybrid Rice Husk/Kenaf Reinforced Polyethylene Terephthalate (PET)/High-Density Polyethylene (HDPE) Blends/Composites

Emmanuel Duniya Kambai[*] [ID], **Inuwa Mohammed Ibrahim, Hauwa M. Mustafa** [ID]

Department of Pure and Applied Chemistry, Faculty of Physical Science, Kaduna State University, Tafawa Balewa Way, PMB 2339, Kaduna, Nigeria
Email: emmifeast@gmail.com

Abstract: Polymer blends offer corrosion resistance, lightweight properties, and toughness, which are vital for fuel economy in the automotive and aerospace sectors. Rice husks and kenaf fiber enhance mechanical and thermal properties, offering cost-effective and eco-friendly reinforcement options. This study aims to incorporate natural fibers such as kenaf and rice husks into a blend of High-Density Polyethylene Blow (HDPEb) and Polyethylene Terephthalate (PET) to fabricate a hybrid composite with enhanced mechanical and thermal properties suitable for automotive applications such as car bumpers. Compression moulding was used for the composite fabrication, while Fourier Transform Infrared (FTIR) spectroscopy, Scanning Electron Microscopy (SEM), and mechanical and thermal properties of the hybrid composite were determined. SEM analysis elucidates the improved dispersion and interfacial adhesion between the rice husk-kenaf fiber (RK) particles and the polymer matrix. Notably, 30% RH/KENAF hybrid composite exhibits commendable mechanical properties, including a tensile strength of 350.19 MPa, elongation at break of 9.92%, impact strength of 0.228 J/m^2, average hardness of 64.8 Hv, flexural strength of 70.43 MPa, flexural modulus of 2,838.86 MPa, and an initial decomposition temperature of 693.50 °C, with a final maximum rate of decomposition reaching 800 °C. The results of this work extend to diverse applications, particularly in the automotive industry, where enhanced materials are sought for applications such as replacement parts and car bumpers.

Keywords: high-density Polyethylene blow (HDPEb), Polyethylene Terephthalate (PET), Kenaf fiber, rice husk filler, hybrid composite, mechanical properties

1. Introduction

Natural fibers offer significant potential as reinforcements in composite materials for various essential human goods, particularly in automotive components, as highlighted in [1]-[3]. While plastics are integral to the automotive industry, providing benefits such as comfort, safety, cost-effectiveness, weight reduction, and design flexibility, their application in vehicle exteriors is notable. Approximately 30% of current car exteriors feature plastic components, replacing traditional heavy steel bumpers and glass headlamp lenses. Plastic parts, affixed with clips or bolts, enhance the vehicle's crash management system, with modern bumper designs incorporating a plastic cover atop a reinforced metal alloy bar [4]-[5].

Hybrid composites, which blend mechanical strength and ecological considerations, potentially surpass single-fiber composites in terms of tensile, flexural, and compressive strength [6]. They also enhance rigidity, resist moisture, and protect against environmental degradation [7]-[10]. Unlike glass-fiber composites, hybrids are more environmentally responsive, cost-effective, and lighter [11]. Incorporating multiple fiber types, hybrid composites balance strength, stiffness, and cost-effectiveness, offering superior properties and economic viability compared with traditional composites.

The global automotive industry aims to achieve 74 million units in sales by 2019, correlating with a rise in road accidents. Small- to medium-scale damages from collisions, constituting 80%, often do not require part replacement. However, synthetic fiber composites, like those with glass fibers, contribute to non-decomposable waste [12]-[13]. Biodegradable polymers like polycaprolactone and poly (butylene succinate) have petroleum origins, whereas traditional fiber-reinforced plastics pose recycling challenges, causing pollution. India, which is reliant on rice, faces environmental issues from burning rice husks. The demand for composite materials has surged, but challenges persist, necessitating innovative, sustainable solutions for cost-effective composites with enhanced mechanical and thermal properties in diverse engineering applications [14].

In the literature review, [15] examined polyester-based hybrid composites with sisal and silk fibers, highlighting the superior mechanical properties of 20 mm fiber lengths and the positive impact of alkali treatment. [16] investigated basalt fiber-based laminates, and found the best performance in basalt/flax-glass composites. [17] explored curaua/ glass composites, emphasizing the improvement in impact strength with glass fiber incorporation. [18] demonstrated enhanced mechanical properties in kenaf/epoxy composites through the synergistic combination of carbon and glass fibers.

The stacking sequence emerged as crucial, affecting the mechanical performance of kenaf/jute/glass composites. [19]-[20] highlighted kevlar as a superior skin layer in hybrid composites. [21]-[23] studied composites of Palmyra fiber waste and glass fibers, noting improved flexural strength. [24] focused on tea leaf particleboard, emphasizing satisfactory physical and mechanical properties.

The growing interest in synthetic fibers for natural fiber composites has been discussed, particularly in kenaf and glass fiber composites [25]. Aramid fibers, like Nomex and Kevlar, were explored for their unique structural properties. [26] investigated hybrid polymer composites, revealing increased Kevlar layers enhancing tensile strength and modulus, indicating the potential for higher modulus-to-density ratios in polymer composites.

Compatibilization enhances the stability of polymer blends by adding a substance, improving the phase morphology for superior mechanical properties. Various tests characterize physical properties [13], [21]. Rice hulls or husks, historically vital in scarcity, find modern applications in building, fertiliser, and insulation. They are abundant and cost-effective, their low thermal conductivity makes them suitable for insulation, and their ash enhances polymer composites [27]-[28].

Kenaf, scientifically Hibiscus cannabinus, part of the Malvaceae family, known as Deccan hemp or Java jute, is an African native plant valued for versatile fibers. Reaching 3 m in height four to five months post-seeding, it adapts to diverse climates [29]. The stem, with bast and core fibers and a central pith layer, comprises 35% bast fiber suitable for paper, textiles, and rope, and 65% core fiber ideal for animal bedding and potting media. Kenaf has gained global attention, akin to jute, for its use in renewable and biodegradable composite materials. The textile industry employs kenaf fiber in polymer matrix composites to enhance flexural strength and impact resistance [30]. Kenaf fiber demonstrates moderate to high tensile strength, ranging from 200 to 1,000 MPa, and is influenced by maturity and processing techniques [31]-[32]. The fibers exhibit good thermal stability (220 to 400 °C), making them suitable for applications like insulation [33]. However, proper moisture management is crucial since kenaf fibers absorb moisture, affecting their mechanical and thermal properties.

Blending Polyethylene Terephthalate (PET) with High Density Polyethylene (HDPE) can create composite materials with improved mechanical and thermal properties. However, there are several drawbacks associated with PET/HDPE blend-based composites: Polyethylene Terephthalate (PET) and High-Density Polyethylene (HDPE) have different chemical structures and properties, leading to poor compatibility between the two polymers. This can result in phase separation and reduced mechanical properties of the composite material [34]. The tensile strength of PET/ HDPE blends-based composites may be lower than that of pure PET or HDPE due to the presence of phase boundaries and interfaces between the two polymers. HDPE has higher thermal stability than PET. Blending PET with HDPE may

result in a composite with reduced thermal stability, especially at elevated temperatures. Achieving uniform dispersion and distribution of HDPE in the PET matrix during the blending process can be challenging. Poor dispersion can lead to variations in the mechanical properties and performance of the composite material. PET is a commonly recycled polymer, but blending it with HDPE may complicate the recycling process. The presence of two different polymers in the composite can hinder efficient separation and recycling [34].

This research aims to capitalize on the benefits of polymer blends, such as corrosion resistance, lightweight properties, and toughness, which are crucial for improving fuel economy in the automotive and aerospace sectors. Rice husks, known for their low density, moisture content, and thermal stability, offer the potential to enhance mechanical and thermal properties, making them suitable for insulation materials. Additionally, kenaf fiber presents itself as a cost-effective and environmentally friendly reinforcement option with desirable mechanical properties. Polyamide (PA or Nylon), Polypropylene (PP), Polyurethane (PU), Acrylonitrile Butadiene Styrene (ABS), and Polybutylene Terephthalate (PBT) are widely utilized plastics in automotive applications, particularly for car bumpers, owing to their commendable mechanical and thermal characteristics. However, concerns regarding cost and environmental impact are associated with their usage [35]-[36]. Conversely, Polyethylene (PE) and Polyethylene Terephthalate (PET) are less favored for car bumper applications due to their inferior mechanical and thermal properties, despite being cost-effective and eco-friendly alternatives [36]. Callister, Consequently, this research endeavors to incorporate natural fibers such as kenaf and rice husks into a blend of Polyethylene Terephthalate (PET) and High-Density Polyethylene (HDPE) to fabricate a hybrid composite with enhanced mechanical and thermal properties suitable for automotive applications like car bumpers.

2. Materials and methods

2.1 *Materials*

Polymer resins or blends, polyethylene terephthalate (PET) and high-density polyethylene (HDPE) blow, kenaf fiber, rice husk particulate filler, compatibilizer (maleic anhydride), and Sodium hydroxide.

2.2 *Sampling*

Polyethylene terephthalate (PET) was acquired from RH Plastic Company located in the PAN Road Industrial Layout, Kaduna State. High-density polyethylene (HDPE) blow was sourced from Mutunchi Plastic Company in Kudenda, Kaduna State. Kenaf, processed and treated, was imported from Bangladesh. The particulate filler, namely rice husk, was obtained from a local milling machine shop, pre-sized to 70 μm. The compatibilizer was procured from Leather Research Zaria. Figure 1 shows the process design of RH/KENAF hybrid composites from sampling to characterization.

2.3 *Alkaline treatment of rice husks*

The rice husks were initially washed with tap water and then air-dried for 48 hours. Subsequently, the husks were ground into a particulate size using a grinding machine and sieved through a 70 μm sieve to achieve a uniform particle size.

For the alkali treatment, 500 g of rice husks were placed in a 5,000 mL beaker with 500 mL of 0.2 M sodium hydroxide (NaOH) solution, which was maintained at 63 °C for 1 hour. The treated material was subsequently washed thoroughly with distilled water and dried in an oven at 105 °C for 48 hours, as documented in [37]-[38].

Similarly, another batch of 500 g of rice husks underwent digestion in a 5,000 mL beaker containing 500 mL of 0.5 M sodium hydroxide (NaOH) solution at 37 °C for 2 hours. Following the digestion, the material was meticulously washed with distilled water and dried in an oven at 105 °C for 48 hours, as reported by [39]-[41], as depicted in Figure 2. The two treated rice husks were homogenously mixed together and used as fillers in the hybrid composite formation.
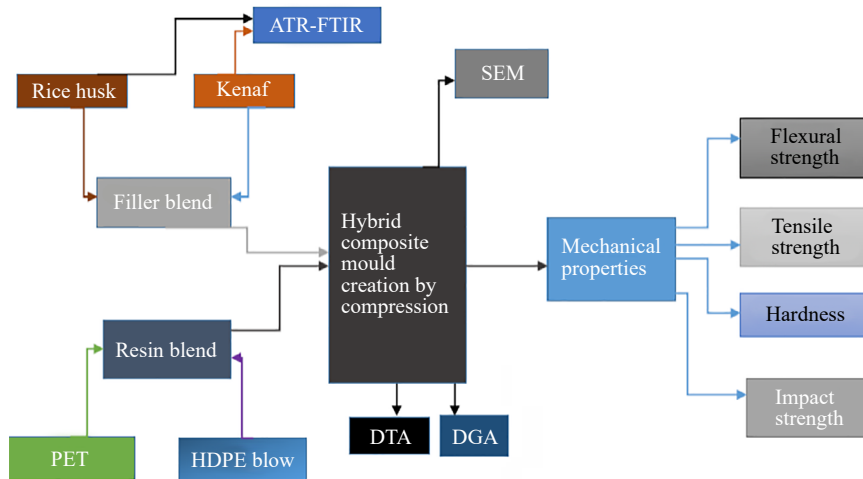
Figure 1. Schematic of the synthesis process of RH/KENAF hybrid composites

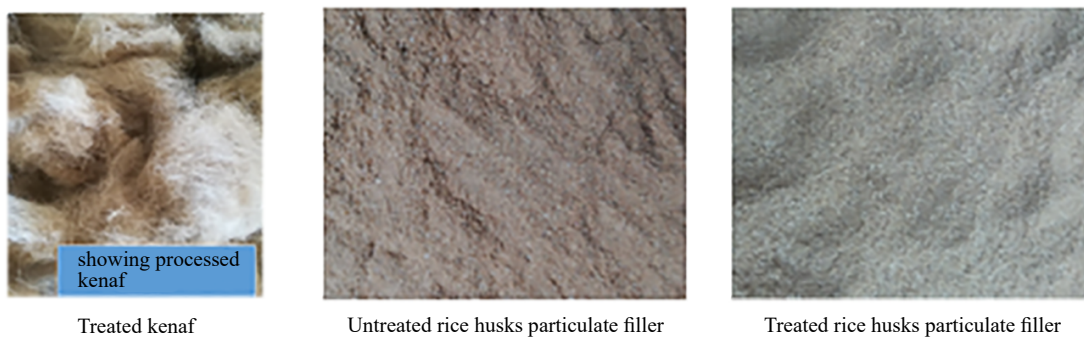| Treated kenaf | Untreated rice husks particulate filler | Treated rice husks particulate filler |

Figure 2. Treated and untreated rice husk and kenaf

2.4 *Functional group analysis*

The structural changes in both rice husks and kenaf were analyzed through infrared (IR) spectroscopy using the Agilent ATR-FTIR instrument. The instrument was powered on, warmed up, and calibrated with specific parameters, including a Sample scan of 30, Background scan of 16, Range of 4,000 cm^{-1} to 650 cm^{-1}, resolution of 8, and system status set to Good. Subsequently, a small amount of each untreated and treated sample was placed on the ATR crystal surface, and the sample compartment was closed securely. The measurement process was initiated, allowing the instrument to collect and generate the infrared spectrum. This spectrum reflects the absorption of infrared light by the functional groups present in both the treated kenaf fiber and the untreated to treated particulate rice husk filler, as depicted in Figure 5. The methodology follows established procedures [42].

2.5 *Preparation of polymer resin composition, filler blend composition, and RH/KENAF hybrid composite*

A polymer resin blend for hybrid composite production was prepared by combining 50% High-Density Polyethylene (HDPE) blow with an equal proportion of Polyethylene Terephthalate (PET) in Table 1. The blending process involved the introduction of pellets of both polymers (PET and HDPE blow) while the mill machine rolls moved in a counter-clockwise motion at a temperature of 170 °C for 5 minutes. This allowed the polymers to soften. After achieving a band and bank formation of the polymer blend on the front roll, a filler blend of treated rice husk (0.2 and 0.5 mixed together) and kenaf, prepared at 30:70 rice husk/kenaf filler content beforehand, was gradually introduced to

the bank. The filler blend underwent cross-mixing and was combined for 3 minutes. The resulting composite was then sheeted out and labeled following the methodology outlined in Figure 3 [43].

Figure 3. Compression moulding machine used for the composite formation

Table 1. Composite composition for PET-HDPEb-rk hybrid composite preparation

Samples	30%:70% Rice Husks/Kenaf	1:1 HDPE/PET Blends
1	0	100 (Control)
2	10	10
3	20	20
4	30	30
5	40	40
6	50	50

A two-roll mill was used for mixing fillers and the polymer blend, Compression Moulding Machine was used for hot pressing at a temperature of 150 °C and pressure of 2.5 MPa for 5 mins [44]. Mechanical property assessments, including hardness, impact, tensile, and flexural tests, were performed on the hybrid composites in accordance with the ASTM standards. The evaluation of Thermo Gravimetric Analysis and Differential Thermal Analysis for the hybrid composites was also conducted, as outlined in the study [43], as depicted in Figure 4.
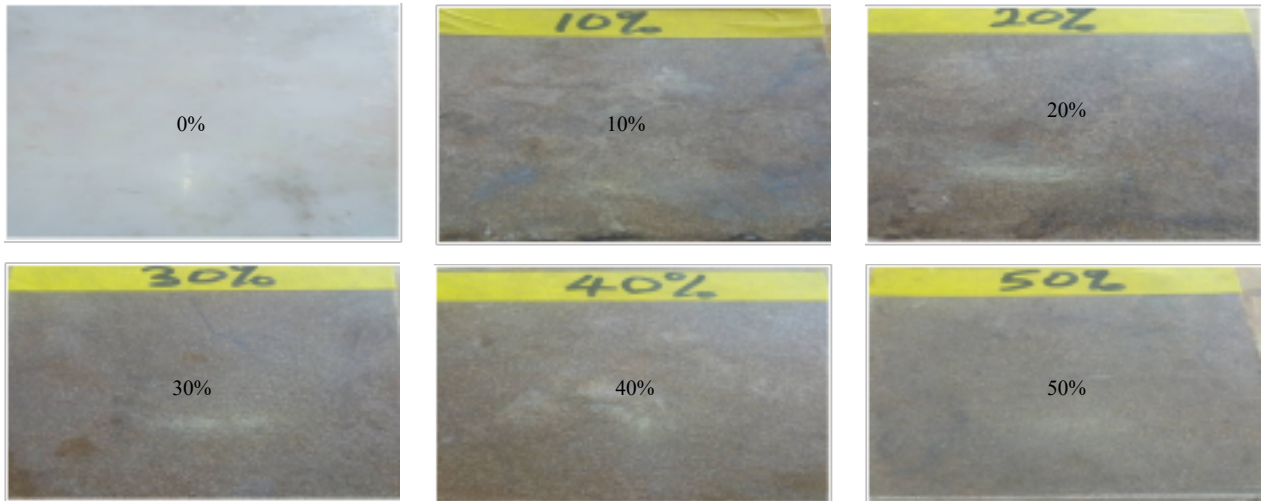
Figure 4. Various RH/KENAF hybrid composite in their percentages of formation

2.6 *Mechanical analysis*

2.6.1 *Tensile strength*

The tensile strength was carried out in accordance with ASTM D-638 [45]-[47].

2.6.2 *Impact strength*

The impact test was carried out according to the standard specified ASTM D-156. The specimen was cut to dimensions 64 mm × 12.7 mm × 3.2 mm and 45° notched was inserted at the middle of the test specimens from all the produced composite samples. The impact energy test was carried out using Izod Impact Tester (Resil impact testing machine). The specimen was clamped vertically on the jaw of the machine and a hammer of weight 1,500 N was released from an inclined angle of 150°. The impact energy for the corresponding tested specimen was measured and recorded [46]-[47]. The impact strength was calculated and recorded accordingly using equations 1 and 2.

$$\text{Average Impact Energy} = \frac{1st + 2nd + 3rd}{3} \text{ (J)} \tag{1}$$

$$\text{Impact Strength} = \frac{Average\ Impact\ Energy}{Sample\ Thickness} \text{ (J/mm)} \tag{2}$$

Sample thickness = 3.2 mm

2.6.3 *Hardness*

The hardness test was carried out in accordance with ASTM D2240 on a Mico Vicker Hardness Tester. The test was carried out at different positions on each sample, and the average hardness was calculated using equation 3.

$$\text{Average Hardness} = \frac{1st + 2nd + 3rd}{3} \text{ (Hv)} \tag{3}$$

2.6.4 *Flexural strength*

The flexural strength test on the blends was carried out in accordance with ASTM D-790. The specimen measuring 100 mm × 25 mm × 3.2 mm was placed on a support span horizontally at 80 mm gauge length and a steady load was applied to the centre by the loading nose, producing three-point bending until the sample specimen failed. The maximum load (N) and the corresponding deflection (mm) were recorded accordingly as the sample specimen failed [46]-[47]. The flexural strength and modulus were calculated using equations 4 and 5, respectively.

$$\text{Flexural Strength} = 3FL / 2bd^2 \text{ (MPa)} \tag{4}$$

$$\text{Flexural Modulus} = FL^3 / 4bd^3D \text{ (MPa)} \tag{5}$$

Where, F = Maximum Load at break, L = distance between the support spans at both edge of the specimen = 80 mm, b = Sample width = 25 mm, and d = Sample thickness = 3.2 mm.

2.7 *Thermo gravimetric analysis (TGA) and differential thermal analysis (DTA)*

Small quantities of the sample were placed onto the sample holder and then placed in the analysis chamber, covered on the chiller, and allowed to cool to 15 °C. All the information about the sample was inputted and the nitrogen was opened to a flow rate of 20 and the analysis was started in accordance with ASTM E1131 [48].

3. Results and discussion

3.1 *ATR-FTIR spectrum of untreated and treated rice husk filler (RHF)*

The analysis of Attenuated Total Reflectance-Fourier Transform Infrared (ATR-FTIR) spectra for diverse specimens, such as kenaf fiber, untreated rice husk as shown in Figure 5, and rice husk treated with varying concentrations of a solution (0.2 M and 0.5 M), revealed crucial vibrational bands associated with cellulose, hemicellulose, and lignin components. In the spectral range of 3,500 to 3,100 cm^{-1}, O-H stretching vibrations display peaks in all samples, indicating hydroxyl group involvement in hydrogen bonding. The peak's breadth suggests a mix of intermolecular and intramolecular hydrogen bonds, providing insights into cellulose crystallinity and the hydrogen bonding network. A faint peak at 2,900 cm^{-1} suggests that the chemical structure of cellulose remains relatively unaltered by treatments, implying minimal changes to alkyl or methylene groups.
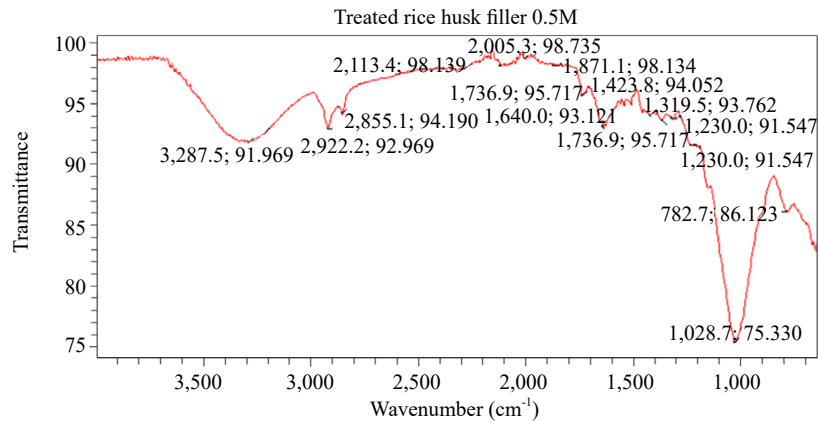

Untreated rice husk filler

Treated rice husk filler 0.2M
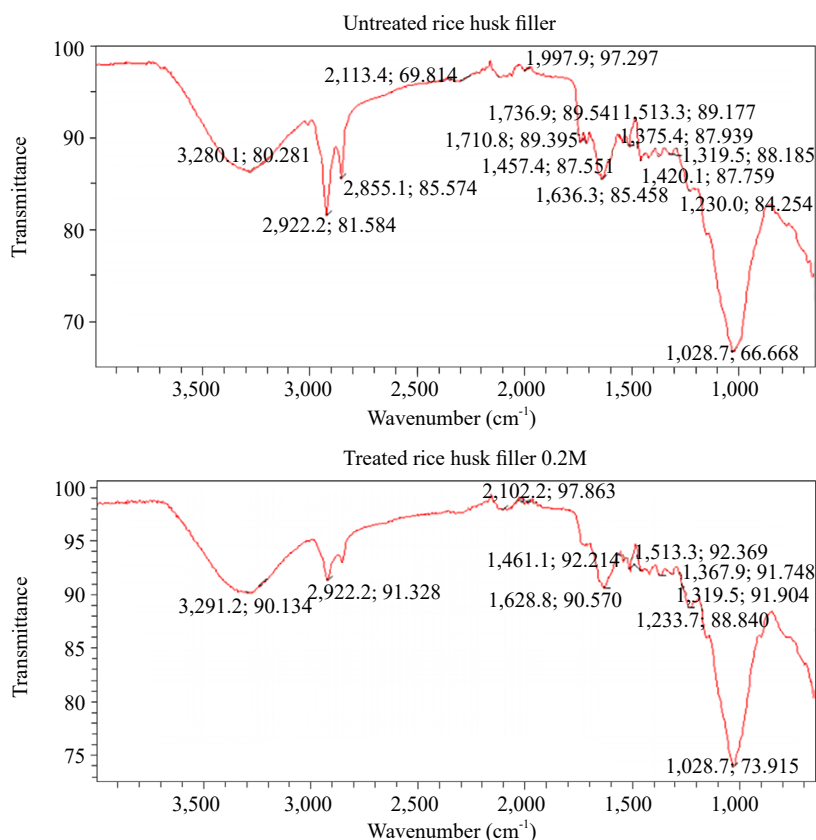
Figure 5. ATR-Fourier transform infrared spectroscopy of rice husk filler: untreated, 0.2 M treated, and 0.5 M treated

Peaks at 1,730 cm^{-1}, associated with C = O stretching vibrations in carbonyl groups, signify potential C-O stretching vibrations in hemicellulose, highlighting its contribution to the sample composition. Peaks in the range of 1,620 to 1,550 cm^{-1} indicate C = C stretching vibrations in aromatic rings, confirming the presence of lignin. Peaks at 1,245 to 1,265 cm^{-1} align with C-O stretching vibrations, which are likely related to glycosidic linkages in cellulose. Peaks in the range of 902 to 870 cm^{-1} indicate alpha glycosidic linkages in cellulose glucose units, persisting across all samples and suggesting minimal impact on the cellulose backbone due to treatments. This aligns with previous research findings, providing a comprehensive understanding of the vibrational characteristics of the analyzed samples [23], [49]-[51]. The research of Inuwa et al. in 2014 [28] correlated observed wavenumber ranges with O-H stretching and O-H bending, along with bands associated with C-H stretching, C = O stretching, benzene skeleton, and C-O stretching vibrations, contributing to a holistic interpretation of the samples' vibrational characteristics.

3.2 *The scanning electron microscopy (SEM) micrographs of the hybrid composites*

SEM 10% of hybrid composite

SEM 30% of hybrid composite
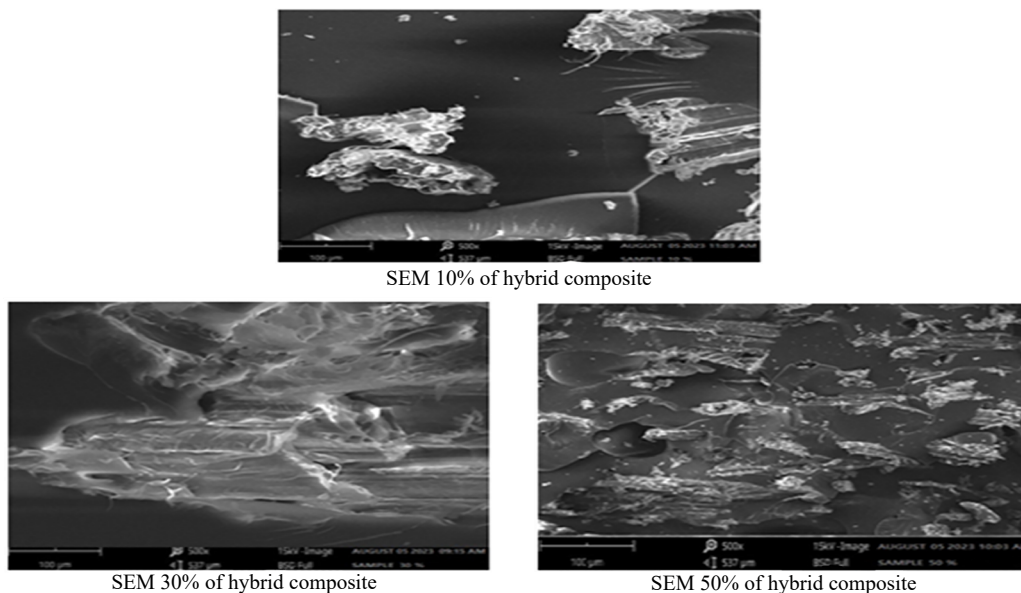
SEM 50% of hybrid composite

Figure 6. SEM micrograph of 10, 30, and 50% RH/KENAF hybrid composite

Figure 6 displays Scanning Electron Microscopy (SEM) micrographs of the RH/KENAF hybrid composite,

revealing insights into the morphology and dispersion of rice husk and kenaf fillers within the polymer matrix. The discussion focuses on the microstructures observed at varying concentrations of RH/KENAF fillers (10%, 30%, and 50%). At 10% RH/KENAF filler concentration, minimal agglomeration of the filler is noted, indicating uneven dispersion due to the lower filler concentration. This non-uniform distribution may enhance composite properties by providing more heterogeneous reinforcement [52].

In the 30% RH/KENAF hybrid composite, SEM micrographs demonstrated a more uniform dispersion of fillers, improving interfacial adhesion and mechanical properties. This optimal loading enhances the overall performance of the composite material, with a balanced distribution of filler particles. Conversely, the 50% composite exhibits increased agglomeration, suggesting that exceeding the optimal loading capacity leads to crowded and less dispersed filler particles. This agglomeration diminishes the reinforcing phase's effectiveness, potentially reducing interfacial interaction and negatively impacting composite performance. Comparable morphologies have been reported by [53] in their studies on different composite materials.

3.3 Mechanical analysis test results

3.3.1 Tensile strength test results

The analysis of tensile strength in hybrid composite materials, as depicted in Figures 7 and 8, reveals a range of values spanning from 17.51 MPa (50% RH/KENAF hybrid composite) to 26.07 MPa (0% RH/KENAF filler). Interestingly, there was an observed decrease in tensile strength with an increase in the RH/KENAF filler percentage, reaching its lowest point at 50% RH/KENAF hybrid composite. Conversely, the highest tensile strength values were noted for the 0% RH/KENAF filler (26.6 MPa) and 30% RH/KENAF hybrid composite (26.07 MPa). Particularly noteworthy is the significant tensile strength of 26.07 MPa observed for the 20% RH/KENAF hybrid composite, while the elastic modulus peaked at 350.19 MPa for the 30% RH/KENAF hybrid composite. This suggests that the 20% and 30% RH/KENAF filler hybrid composites offer an optimal balance of strength and stiffness.
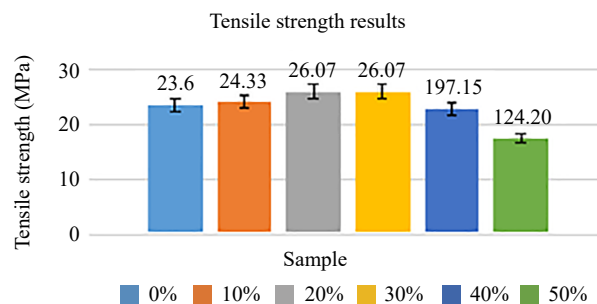
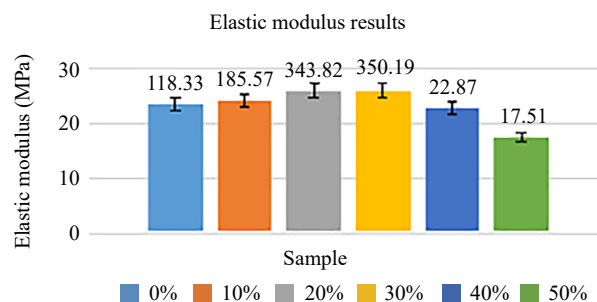**Figure 7.** Tensile strength of prepared RH/KENAF hybrid composite

Figure 8. Elastic modulus of prepared RH/KENAF hybrid composite

In contrast, the 0% RH/KENAF filler and 10% RH/KENAF hybrid composites exhibited higher elongation break

Engineering Science & Technology

values, likely due to the limited filler content. This study implies that excessive RH/KENAF filler percentages (40% and 50%) may have a detrimental effect on mechanical properties, indicating an optimal filler range for composite materials. This finding is consistent with previous research [9]. The latter study also reported similar trends, where the addition of 5% SEBS-g-MA (phr) increased tensile strength, but the effect diminished with higher SEBS-g-MA (phr) concentrations, aligning with the findings of [54] regarding the impact of SEBS-g-MA on the mechanical properties of PA6/PP/OMMT nanocomposites. These observations underscore the importance of carefully selecting and optimizing blend compositions to achieve the desired mechanical properties in hybrid composite materials.

3.3.2 Impact strength test results

The impact strength analysis of the RH/KENAF hybrid composite material in Figure 9 revealed intriguing patterns across different percentages of the RH/KENAF filler. Starting from 0% RH/KENAF filler, the impact strength stood at 0.273 J/mm, gradually declining to 0.205 J/mm at 10% RH/KENAF hybrid composite. Remarkably, it stabilized at 0.218 J/mm for 20% RH/KENAF hybrid composite, showed a slight increment to 0.228 J/mm at 30% RH/KENAF hybrid composite, followed by a decrease to 0.199 J/mm at 40% RH/KENAF hybrid composite, and further to 0.182 J/mm at 50% RH/KENAF hybrid composite. This observed decreasing trend is consistent with prior research [9], which is common in composite materials where the introduction of blends affects energy absorption. However, an exception emerged at 30% RH/KENAF hybrid composite, suggesting a temporary enhancement in mechanical properties due to a unique interaction. Several potential reasons can elucidate the observed trend, including filler dispersion, fiber alignment, and matrix-filler interaction. [9] reported similar results, where a 10% SEBS-g-MA (phr) exhibited the highest impact strength, but the strength decreased with a rise in SEBS-g-MA (phr) to 20%. This finding aligns with the observations of [12], [49], who noted that a 3% GNP (phr) blend demonstrated the highest impact strength, which diminished with an increase in the GNP (phr) blend to 5%. Overall, the impact strength analysis of the Polyethylene Terephthalate (PET)-High-Density Polyethylene Blow (HDPEb-rk) hybrid composite material underscores the complex interplay between blend composition, filler characteristics, and mechanical properties. Understanding these interactions is crucial for optimizing composite formulations to achieve the desired performance characteristics in various applications, including automotive components, construction materials, and consumer products.
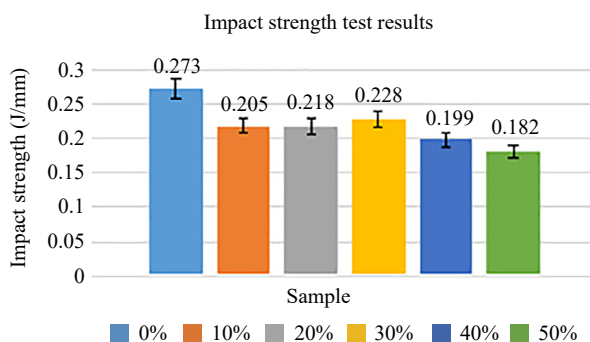

Figure 9. Impact strength of prepared RH/KENAF hybrid composite

3.3.3 Hardness test results

The data presented in Figure 10 illustrates the mean hardness values of a hybrid composite material with varying percentages of RH/KENAF filler. The hardness values ranged from 56.0 Hv at 0% RH/KENAF filler to 64.8 Hv at 30% RH/KENAF hybrid composite. However, a decline was observed at 40% RH/KENAF hybrid composite (64.4 Hv), followed by a substantial drop at 50% RH/KENAF hybrid composite (59.2 Hv). The positive correlation between blend percentage and hardness up to 30% suggests reinforcing effects within the composite material. This phenomenon is attributed to effective filler dispersion and strong interaction between the matrix and fillers. The peak hardness observed at 30% RH/KENAF hybrid composite indicates an optimal concentration of RH/KENAF filler, where the reinforcing

effects are maximized. Beyond 30% RH/KENAF filler, disparities in hardness arise due to several factors. These include a less uniform filler distribution within the matrix, reduced compatibility between the matrix and fillers, and the onset of a saturation effect. The decrease in hardness beyond the optimal concentration challenges further improvement in the mechanical properties. The findings of this study align with the related literature on composite materials. Several studies have reported similar trends in hardness with varying filler content [55].
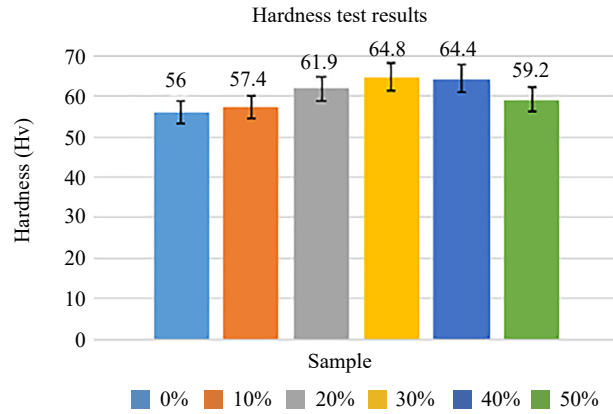

Figure 10. Hardness test results of prepared RH/KENAF hybrid composite
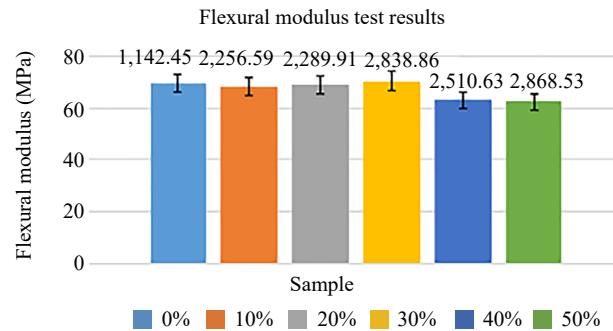
3.3.4 *Flexural strength test results*

Figure 11. Flexural modulus of the RH/KENAF hybrid composite
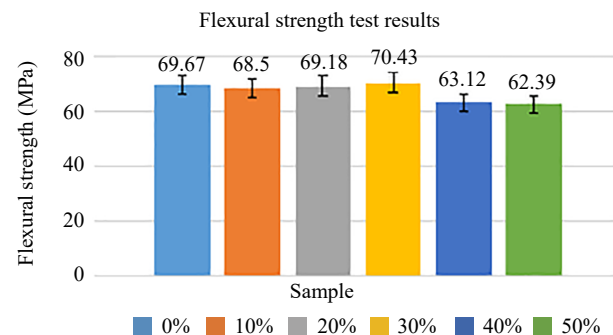

Figure 12. Flexural strength of the RH/KENAF hybrid composite

The flexural strength test is a critical measure of a material's ability to resist bending forces. Figures 11 and 12 present data illustrating the impact of varying blend percentages on a hybrid composite material. The control, consisting of a 0% RH/KENAF filler, demonstrated a flexural strength of 69.67 MPa. A minor decrease to 68.5 MPa occurred at a 10% RH/KENAF hybrid composite, while the strength remained relatively stable at 69.18 MPa for a 20% RH/KENAF hybrid composite. Interestingly, a peak flexural strength of 70.43 MPa was observed at a 30% RH/KENAF hybrid composite, indicating an optimal interaction between the filler and the matrix. However, a notable decline to 63.12 MPa at 40% RH/KENAF hybrid composite and 62.39 MPa at 50% RH/KENAF hybrid composite suggests diminishing returns at higher concentrations.

This decline implies that while a balanced filler-matrix relationship at 30% RH/KENAF hybrid composite enhances flexural strength, higher concentrations may lead to agglomeration and saturation effects. These effects weaken regions within the material, resulting in reduced strength. These findings are consistent with those of previous research [9], [49], which observed similar trends in flexural strength concerning blend percentages. Additionally, [55] reported comparable results, supporting the hypothesis of saturation effects at higher blend percentages. The flexural strength of hybrid composite materials is significantly influenced by the blend percentages of RH/KENAF filler. The data suggest an optimal ratio of 30% RH/KENAF filler for maximizing flexural strength, while higher concentrations may lead to diminished performance due to agglomeration and saturation effects. These findings have important implications for the design and optimization of composite materials for various applications, including automotive components and structural elements.

3.4 *Thermo gravimetric analysis (TGA) and differential thermal analysis (DTA)*

The thermogravimetric analysis (TGA) and derivative thermograms (DTG) of the RH/KENAF hybrid composite are presented in Figures 13, 14, and 15. The 10% RH/KENAF hybrid composite showed an initial decomposition temperature of 230.30 °C, with the maximum rate of decomposition at 705.2 °C and an 84% weight loss. The gradual weight loss at 10% RH/KENAF hybrid composite indicated inadequate thermal stability. The addition of RH/KENAF filler improved thermal stability, with 30% RH/KENAF filler displaying an initial decomposition temperature of 693.50 °C and a final maximum rate of 800 °C. However, the 50% RH/KENAF hybrid composite exhibited a reduced initial decomposition temperature (277.30 °C) compared to the 30% RH/KENAF hybrid composite, although the final decomposing temperature increased by 105.0 °C, starting at a 45% weight loss. Augmented thermal stability resulted from the interaction between the filler blend and resin blend, as observed in the SEM micrographs of the 30% RH/ KENAF hybrid composite.

Conversely, the 10% RH/KENAF hybrid composite displayed diminished thermal stability due to limited interaction, while the reduced stability in the 50% RH/KENAF hybrid composite was attributed to oversaturation. The Differential Thermal Analysis (DTA) in Figures 16, 17, and 18 confirmed a consistent pattern of thermal stability influenced by the composition. Previous studies supported this, revealing that the optimal balance was achieved at 30% RH/KENAF hybrid composite. SEM micrographs further clarified the increased thermal stability due to interactions between the filler blend and resin blend. It is noteworthy that the findings align with the observations of [9], which emphasize the crucial role of blend interaction in determining the thermal properties of hybrid composites. The oversaturation of the RH/KENAF hybrid composite in the 50% composition highlights the delicate balance required to achieve enhanced thermal stability without compromising the overall composition. These insights contribute to the growing body of knowledge on the thermogravimetric behaviour of hybrid composites, offering valuable information for optimizing their thermal performance in various applications. The TGA and DTA results of the RH/KENAF hybrid composite reveal a nuanced relationship between composition and thermal stability. The interplay between Polyethylene Terephthalate (PET)/High-Density Polyethylene Blow (HDPEb) blend and (rk) filler significantly influences the initial decomposition temperature and the overall thermal stability of the hybrid composite. The SEM micrographs provide visual evidence of the interaction, supporting the observed trends in the TGA and DTA analyses. These findings provide valuable insights into the design and optimization of hybrid composites for enhanced thermal performance in diverse applications.
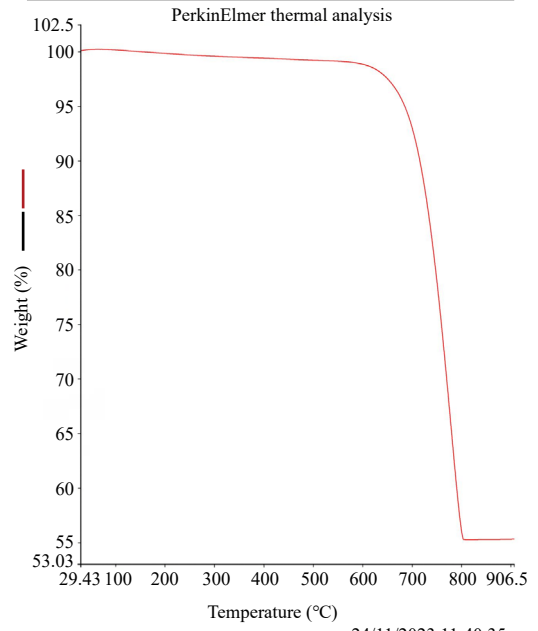
Filename: C:\Users\Administrator\Desktop\T...\10%.t6d
Operator ID: Abdulrahman
Sample ID: 10%
Sample Weight: 20.933 mg
Comment: TGA

PerkinElmer thermal analysis

24/11/2023 10:38:22
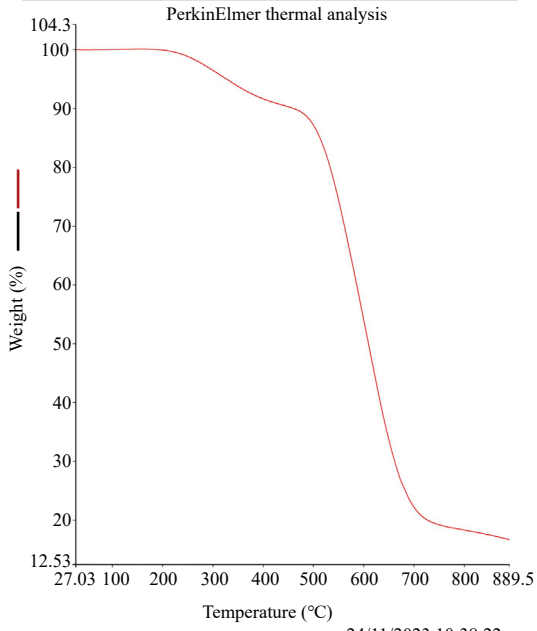
1) Heat from 30.00 °C to 950.00 °C at 10.00 °C/min

Figure 13. Thermo gravimetric analysis of 10% RH/KENAF hybrid composite

Filename: C:\Users\Administrator\Desktop\T...\30%.t6d
Operator ID: Abdulrahman
Sample ID: 30%
Sample Weight: 20.523 mg
Comment: TGA

PerkinElmer thermal analysis

24/11/2023 11:40:35

1) Heat from 30.00 °C to 950.00 °C at 10.00 °C/min

Figure 14. Thermo gravimetric analysis of 30% RH/KENAF hybrid composite

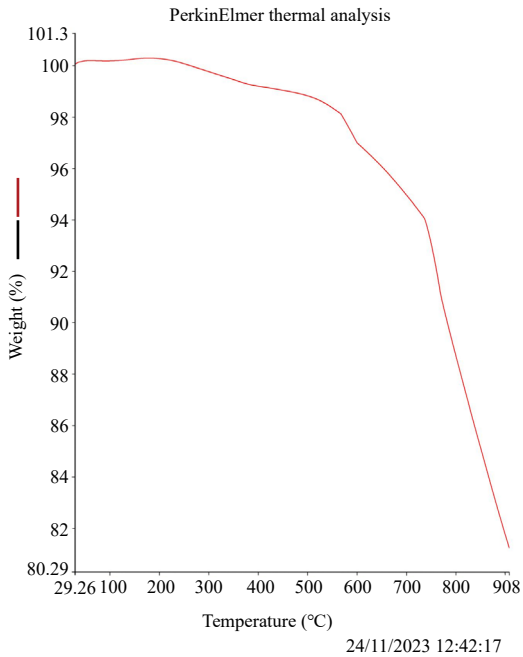Filename: C:\Users\Administrator\Desktop\T...\50%.t6d
Operator ID: Abdulrahman
Sample ID: 50%
Sample Weight: 20.171 mg
Comment: TGA

PerkinElmer thermal analysis

24/11/2023 12:42:17

1) Heat from 30.00 °C to 950.00 °C at 10.00 °C/min

Figure 15. Thermo gravimetric analysis of 50% RH/KENAF hybrid composite

Filename: C:\Users\Administrator\Desktop\T...\10%.t6d
Operator ID: Abdulrahman
Sample ID: 10%
Sample Weight: 20.933 mg
Comment: TGA/DTA

PerkinElmer thermal analysis

24/11/2023 10:39:39

1) Heat from 30.00 °C to 950.00 °C at 10.00 °C/min

Figure 16. Differential thermal analysis for 10% RH/KENAF hybrid composite curve

Filename: C:\Users\Administrator\Desktop\T...\30%.t6d
Operator ID: Abdulrahman
Sample ID: 30%
Sample Weight: 20.523 mg
Comment: TGA/DTA

PerkinElmer thermal analysis

1) Heat from 30.00 °C to 950.00 °C at 10.00 °C/min
24/11/2023 11:40:35

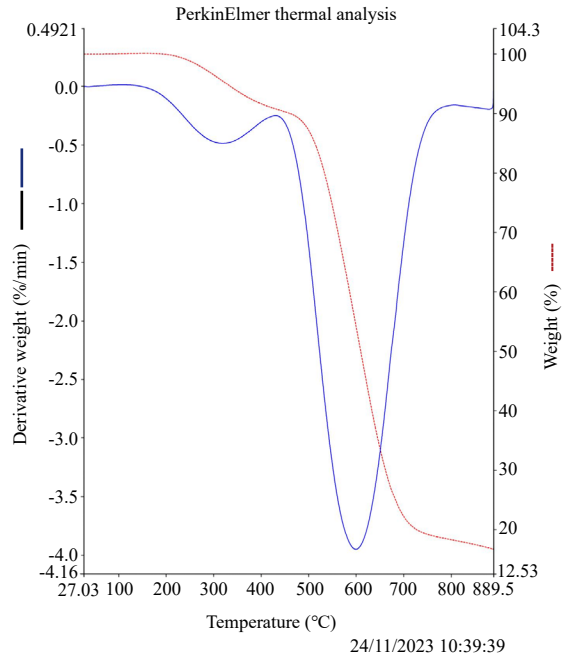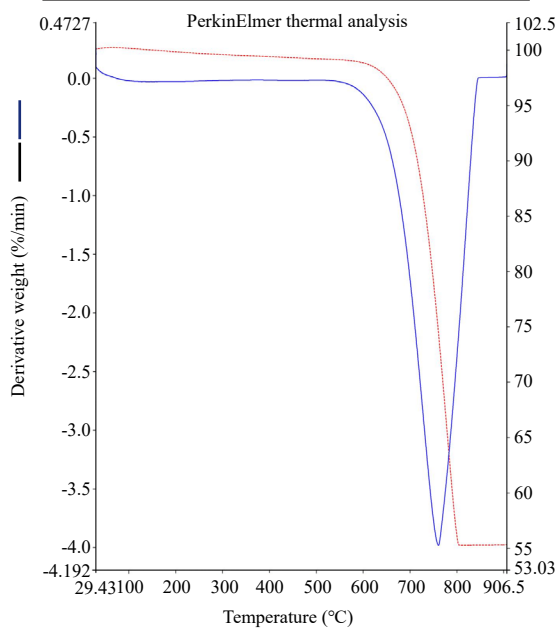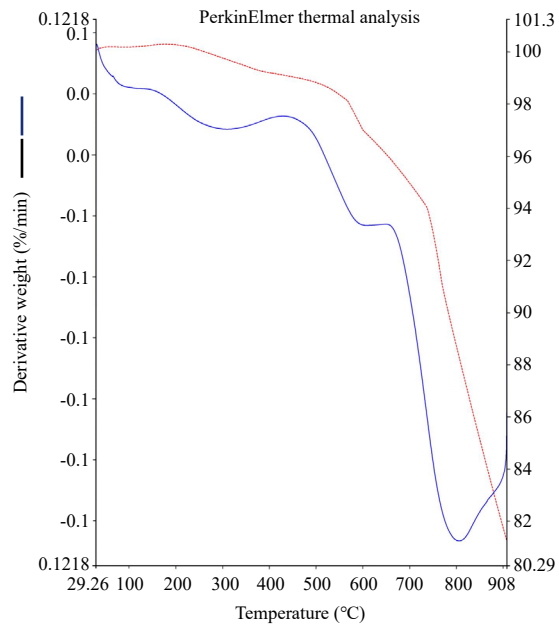**Figure 17.** Differential thermal analysis for 30% RH/KENAF hybrid composite curve

Filename: C:\Users\Administrator\Desktop\T...\50%.t6d
Operator ID: Abdulrahman
Sample ID: 50%
Sample Weight: 20.171 mg
Comment: TGA/DTA

PerkinElmer thermal analysis

1) Heat from 30.00 °C to 950.00 °C at 10.00 °C/min
24/11/2023 12:42:17

Figure 18. Differential thermal analysis for 50% RH/KENAF hybrid composite curve

5. Conclusion

An in-depth analysis of ATR-FTIR spectra was conducted on diverse specimens, namely kenaf fiber, untreated rice husk, and rice husk treated with varying solution concentrations. The examination of vibrational bands provided valuable insights into the cellulose, hemicellulose, and lignin constituents. The primary focus was on the 30% RH/ KENAF hybrid composite, where the FTIR results indicated minimal alteration in the cellulose structure, signifying the preservation of its backbone.

SEM micrographs of the RH/KENAF hybrid composite revealed that at 10% RH/KENAF filler concentration, agglomeration occurred, which was attributed to uneven filler dispersion. Conversely, at 30% RH/KENAF filler concentration, uniform dispersion and improved interfacial adhesion were observed, contributing to the enhanced mechanical properties. However, at 50% RH/KENAF filler concentration, increased agglomeration negatively impacted the overall performance. The mechanical analysis centred on tensile strength, impact strength, hardness, and flexural strength. Tensile strength decreased with increasing Polyethylene Terephthalate (PET)/High-Density Polyethylene Blow (HDPEb) blend, peaking at 30% RH/KENAF filler concentration. Elastic modulus indicated optimal strength and stiffness at 20% and 30% RH/KENAF filler concentration. Impact strength generally declined, with an exception at 30%, suggesting a specific filler-matrix interaction. Hardness showed a positive correlation up to 30% RH/KENAF filler concentration, indicating an optimum concentration for improvement. Flexural strength peaked at 30%, signifying a balanced interaction, but declined beyond 30% RH/KENAF filler concentration.

Thermo gravimetric analysis (TGA) and differential thermal analysis (DTA) unveiled insights into thermal stability, with results indicating the significant influence of composition. SEM micrographs supported these findings, highlighting the interactions between filler and resin blends. The comprehensive analysis underscored the importance of optimizing filler dispersion and matrix interaction for enhancing mechanical and thermal performance. The 30% RH/KENAF hybrid composite emerged as critical, showcasing improved properties across analyses, and contributing valuable insights for designing materials with enhanced characteristics in diverse applications, including car bumper

replacements.

Availability of data

Data availability is not applicable.

Funding

Conflicts of interest

No conflict of interest was associated with this work.

References

[1] M. Fitri and S. Mahzan, "The mechanical properties requirement for polymer composite automotive parts-A review," *International Journal of Advanced Technology in Mechanical, Mechatronics and Materials*, vol. 1, no. 3, pp. 125-133, 2020.

[2] H. L. Huang, C. Y. Li, and Q. Zeng, "Crash protectiveness to occupant injury and vehicle damage: An investigation on major car brands," *Accident Analysis and Prevention*, vol. 86, pp. 129-136, 2016.

[3] A. Gnatov and S. Argun, "New method of car body panel external straightening: tools of method," *International Journal of Vehicular Technology*, vol. 2015, pp. 192958, 2015.

[4] J. G. Drobny, *Handbook of Thermoplastic Elastomers*. Oxford, UK: Elsevier Science, 2014.

[5] O. Osokoya, "An evaluation of polymer composites for car bumper Beam," *International Journal of Automotive Composites*, vol. 3, no. 1, pp. 44-60, 2017.

[6] G. Belingardi, A. T. Beyene, E. G. Koricho, and B. Martorana, "Alternative lightweight materials and component manufacturing technologies for vehicle frontal bumper beam," *Composite Structures*, vol. 120, pp. 483-495, 2015. Available: https://doi.org/10.1016/j.compstruct.2014.10.007.

[7] R. Kozłowski and M. Władyka-Przybylak, "Review flammability and fire resistance of composites reinforced by natural fibers," *Polymers for Advanced Technologies*, vol. 19, no. 6, pp. 446-453, 2008.

[8] S. Kalia, B. S. Kaith, and I. Kaur, "Pretreatments of natural fibers and their application as reinforcing material in polymer composites-A review," *Polymer Engineering & Science*, vol. 49, no. 7, pp. 1253-1272, 2009.

[9] N. A. Jamaludin, I. M. Inuwa, A. Hassan, N. Othman, and M. Jawaid, "Mechanical and thermal properties of SEBS-g-MA compatibilized halloysite nanotubes reinforced polyethylene terephthalate/polycarbonate/ nanocomposites," *Journal of Applied Polymer Science*, vol. 132, no. 39, pp. 42608, 2015.

[10] D. B. Dittenber and H. V. S. Gangarao, "Critical review of recent publications on use of natural composites in infrastructure," *Composites Part A: Applied Science and Manufacturing*, vol. 43, no. 8, pp. 1419-1429, 2012.

[11] H. P. S. A. Khalil, M. S. Alwani, and A. K. M. Omar, "Chemical composition, anatomy, lignin distribution, and cell wall structure of malaysian plant waste fibers," *BioResources*, vol. 1, no. 2, pp. 220-232, 2006.

[12] I. M. Inuwa, A. Hassan, S. A. Samsudin, M. K. M. Haafiz, and M. Jawaid, "Interface modification of compatibilized polyethylene terephthalate/polypropylene blends: Effect of compatibilization on thermomechanical properties and thermal stability," *Journal of Vinyl and Additive Technology*, vol. 23, no. 1, pp. 45-54, 2017.

[13] I. M. Inuwa, A. Hassan, S. A. Samsudin, M. K. M. Haafiz, M. Jawaid, K. Majeed, and N. C. A. Razak, "Characterization and mechanical properties of exfoliated graphite nanoplatelets reinforced polyethylene terephthalate/polypropylene composites," *Journal of Applied Polymer Science*, vol. 131, no. 15, pp. 45082, 2014.

[14] S. Ghosh, J. K. Sinha, S. Ghosh, K. Vashisth, S. Han, and R. Bhaskar, "Microplastics as an emerging threat to the global environment and human health," *Sustainability*, vol. 15, no. 14, pp. 10821, 2023.

[15] P. N. Khanam, M. Mohan Reddy, K. Raghu, K. John, and S. Venkata Naidu, "Tensile flexural and compressive

properties of sisal/silk hybrid composites," *Journal of Reinforced Plastics and Composites*, vol. 26, no. 10, pp. 1065-1070, 2007.

[16] R. Petrucci, C. Santulli, D. Puglia, F. Sarasini, L. Torre, and J. M. Kenny, "Mechanical characterisation of hybrid composite laminates based on basalt fibers in combination with flax, hemp and glass fibers manufactured by vacuum infusion," *Materials & Design*, vol. 49, pp. 728-735, 2013.

[17] J. H. S. Almeida Júnior, S. C. Amico, E. C. Botelho, and F. D. R. Amado, "Hybridization effect on the mechanical properties of curaua/glass fiber composites," *Composites Part B: Engineering*, vol. 55, pp. 492-497, 2013.

[18] C. X. Wang, H. B. Bi, Q. Z. Lin, X. D. Jiang, and C. L. Jiang, "Co-pyrolysis of sewage sludge and rice husk by TGeFTIReMS: Pyrolysis behavior, kinetics, and condensable/non-condensable gases characteristics," *Renewable Energy*, vol. 160, pp. 1048-1066, 2020.

[19] M. R. Sanjay, G. R. Arpitha, P. Senthamaraikannan, M. Kathiresan, M. A. Saibalaji, and B. Yogesha, "The hybrid effect of jute/kenaf/e-glass woven fabric epoxy composites for medium load applications: Impact, inter-laminar strength, and failure surface characterization," *Journal of Natural Fibers*, vol. 16, no. 4, pp. 600-612, 2019.

[20] R. Yahaya, S. M. Sapuan, M. Jawaid, Z. Leman, and E. S. Zainudin, "Effect of layering sequence and chemical treatment on the mechanical properties of woven kenaf-aramid hybrid laminated composites," *Materials & Design*, vol. 67, pp. 173-179, 2015.

[21] R. Velmurgan and V. Manikandan, "Mechanical properties of glass/palmyra fiber waste sandwich composites," *Indian Journal of Engineering & Material Sciences*, vol. 12, no. 6, pp. 563-570, 2005.

[22] R. Yahaya, S. M. Sapuan, M. Jawaid, Z. Leman, and E. S. Zainudin, "Mechanical performance of woven kenaf-Kevlar hybrid composites," *Journal of Reinforced Plastics and Composites*, vol. 33, no. 24, pp. 2242-2254, 2014.

[23] N. I. Abdul Razak, N. A. Ibrahim, N. Zainuddin, M. Rayung, and W. Z. Saad, "The influence of chemical surface modification of kenaf fiber using hydrogen peroxide on the mechanical properties of biodegradable kenaf fiber/poly (Lactic Acid) composites," *Molecules*, vol. 19, no. 3, pp. 2957-2968, 2014.

[24] K. Singh, D. Das, R. K. Nayak, S. Khandai, R. Kumar, and B. C. Routara, "Effect of silanizion on mechanical and tribological properties of kenaf-carbon and kenaf-glass hybrid polymer composites," *Materials Today: Proceedings*, vol. 26, pp. 2094-2098, 2020. Available: https://doi.org/10.1016/j.matpr.2020.02.452.

[25] S. N. Z. Ahmad Nadzri, M. T. Hameed Sultan, A. U. Md Shah, S. N. A. Safri, and A. A. Basri, "A review on the kenaf/glass hybrid composites with limitations on mechanical and low velocity impact properties," *Polymers*, vol. 12, no. 6, pp. 1285, 2020.

[26] H. Bhanupratap and H. C. Chittappa, "Study of tensile behaviour by variation of kevlar to the jute fiber epoxy hybrid composites," *International Journal of Engineering Research & Technology*, vol. 6, no. 6, pp. 1039-1043, 2017.

[27] E. L. Arumingtyas, "Kenaf: its prospect in Indonesia," *Journal of Biological Researches*, vol. 20, no. 2, pp. 21-26, 2015.

[28] I. M. Inuwa, A. Hassan, S. A. Samsudin, M. K. M. Haafiz, A. N. Ibrahim, S. L. Wong, and K. Majeed, "Enhanced mechanical and thermal properties of hybrid graphene nanoplatelets/multiwall carbon nanotubes reinforced polyethylene terephthalate nanocomposites," *Fibers and Polymers*, vol. 17, no. 10, pp. 1657-1666, 2016.

[29] H. M. Akil, M. F. Omar, A. A. M. Mazuki, S. Safiee, Z. A. M. Ishak, and B. A. Abu, "Kenaf fiber reinforced composites: A review," *Materials and Design*, vol. 32, no. 8-9, pp. 4107-4121, 2011.

[30] S. A. Mutasher, A. Poh, A. M. Than, and J. Law, "The effect of alkali treatment mechanical properties of kenaf fiber epoxy composite," *Key Engineering Materials*, vol. 471-472, pp. 191-196, 2011. Available: https://doi.org/10.4028/www.scientific.net/KEM.471-472.191.

[31] A. K. Mohanty, M. Misra, and L. T. Drzal, "Sustainable bio-composites from renewable resources: Opportunities and challenges in the green materials world," *Journal of Polymers and the Environment*, vol. 10, pp. 19-26, 2002.

[32] S. Biswas, S. Kindo, and A. Patnaik, "Effect of fiber length on mechanical behavior of coir fiber reinforced epoxy composites," *Fibers and Polymers*, vol. 12, pp. 73-78, 2011. Available: https://doi.org/10.1007/s12221-011-0073-9.

[33] R. M. N. Arib, S. M. Sapuan, M. M. H. M. Ahmad, M. T. Paridah, and H. M. D. Khairul Zaman, "Mechanical properties of pineapple leaf fiber reinforced polypropylene composites," *Materials and Design*, vol. 27, no. 5, pp. 391-396, 2006.

[34] M. Olam, "Mechanical and thermal properties of HDPE/PET microplastics, applications, and impact on environment and life," in *Advances and Challenges in Microplastics*, E. S. Salama, Ed. London: Intechopen, 2023.

[35] T. A. Osswald and G. Menges, *Materials Science of Polymers for Engineers*. 3rd ed., Munich, Germany: Hanser Publications, 2008.

[36] W. D. Callister and D. G. Rethwisch, *Materials Science and Engineering: An Introduction*. 10th ed., New York:

John Wiley & Sons, 2018.

[37] H. Jaya, M. F. Omar, H. M. Akil, Z. A. Ahmad, and N. N. Zulkepli, "Effect of particle size on mechanical properties of sawdusthigh density polyethylene composites under various strain rates," *BioResources*, vol. 11, no. 3, pp. 6489-6504, 2016.

[38] I. Z. Luna, K. C. Dam, A. M. Sarwaruddin Chowdhury, Md. Abdul Gafur, N. Khan, and R. A. Khan, "Physical and thermal characterization of alkali treated rice husk reinforced polypropylene composites," *Advances in Materials Science and Engineering*, vol. 2015, pp. 907327, 2015. Available: https://doi.org/10.1155/2015/907327.

[39] M. Mareya, A. Bahurudeen, J. Varghese, B. S. Thomas, and N. T. Sithole, "Transformation of rice husk modified basic oxygen furnace slag into geopolymer composites," *Journal of Materials Research and Technology*, vol. 24, pp. 6264-6278, 2023. Available: https://doi.org/10.1016/j.jmrt.2023.04.225.

[40] M. N. Islam and M. I. Sakinul, "Mechanical properties of chemically treated sawdust-reinforced recycled polyethylene composites," *Industrial & Engineering Chemistry Research*, vol. 50, no. 19, pp. 11124-11129, 2011.

[41] U. Kumar and M. Bandyopadhyay, "Sorption of cadmium from aqueous solution using pretreated rice husk," *Bioresource Technology*, vol. 97, no. 1, pp. 104-109, 2006.

[42] N. D. Aliyu, G. Wyasu, B. Myek, and J. B. Yakasai, "Green synthesis of eco-friendly potasium nanoparticles and its application on Amarathus viridis, solanum lycopersocum and hibiscussabdariffa plants," *Science World Journal*, vol. 18, no. 3, pp. 485-491, 2023.

[43] H. C. Chen, T. Y. Chen, and C. H. Hsu, "Effects of wood particle size and mixing ratios of HDPE on the properties of the composites," *European Journal of Wood and Wood Products*, vol. 64, no. 3, pp. 172-177, 2006.

[44] Z. J. Gombos, P. McCutchion, and L. Savage, "Thermo-mechanical behaviour of composite moulding compounds at elevated temperatures," *Composites Part B: Engineering*, vol. 173, pp. 106921, 2019. Available: https://doi.org/10.1016/j.compositesb.2019.106921.

[45] ASTM Committee D20, *Standard Test Method for Tensile Properties of Plastics Mechanical Properties*. United States: ASTM International, 2010.

[46] Y. Dan-mallam, M. Z. Abdullah, and P. S. M. Megat Yusoff, "The effect of hybridization on mechanical properties of woven kenaf fiber reinforced polyoxymethylene composite," *Polymer Composites*, vol. 35, no. 10, pp. 1900-1910, 2014.

[47] S. R. Sachin, A. M. Kuzmin, S. Krishnakumar, S. Saravanan, and T. K. Kannan, "Philosophy of selecting ASTM standards for mechanical characterization of polymers and polymer composites," *Materiale Plastice*, vol. 58, no. 3, pp. 247-256, 2021.

[48] R. Bottom, "Thermogravimetric analysis," in *Principles and Applications of Thermal Analysis*, P. Gabbott, ed. Hoboken, NY: Blackwell Publishing, 2008, pp. 87-118.

[49] I. M. Inuwa, A. Hassan, S. A. Samsudin, H. M. Mohamad Kassim, and M. Jawaid, "Mechanical and thermal properties of exfoliated graphite nanoplatelets reinforced polyethylene terephthalate/polypropylene composites," *Polymer Composites*, vol. 35, no. 10, pp. 2029-2035, 2014.

[50] M. S. Mohd Basri, F. Mustapha, N. Mazlan, and M. R. Ishak, "Rice husk ash-based geopolymer binder: Compressive strength, optimize composition, FTIR spectroscopy, microstructural, and potential as fire-retardant material," *Polymers*, vol. 13, no. 24, pp. 4373, 2021.

[51] D. L. Majid, Q. M. Jamal, and N. H. Manan, "Low-velocity impact performance of glass fiber, kenaf fiber, and hybrid glass/kenaf fiber reinforced epoxy composite laminates," *BioResources*, vol. 13, no. 4, pp. 8839-8852, 2018.

[52] T. Ramanathan, S. Stankovich, D. A. Dikin, H. Liu, H. Shen, S. T. Nguyen, and L. C. Brinson, "Graphitic nanofillers in PMMA nanocomposites-An investigation of particle size and dispersion and their influence on nanocomposite properties," *Journal of Polymer Science Part B: Polymer Physics*, vol. 45, no. 15, pp. 2097-2112, 2007.

[53] X. Jiang and L. T. Drzal, "Multifunctional high density polyethylene nanocomposites produced by incorporation of exfoliated graphite nanoplatelets 1: Morphology and mechanical properties," *Polymer Composites*, vol. 31, no. 6, pp. 1091-1098, 2010.

[54] Z. A. M. Ishak, W. S. Chow, and T. Takeichi, "Influence of SEBS-g-MA on morphology, mechanical, and thermal properties of PA6/PP/organoclay nanocomposites," *European Polymer Journal*, vol. 44, no. 4, pp. 1023-1039, 2008.

[55] K. Kalaitzidou, H. Fukushima, H. Miyagawa, and L. T. Drzal, "Flexural and tensile moduli of polypropylene nanocomposites and comparison of experimental data to Halpin-Tsai and Tandon-Weng models," *Polymer Engineering & Science*, vol. 47, no. 11, pp. 1796-1803, 2007.